

## Galley Proof Corrections Checklist

Dear Author,

To avoid commonly occurring errors, please ensure that the following important items are correct in your proofs (please note that once your article is published online, no further corrections can be made):

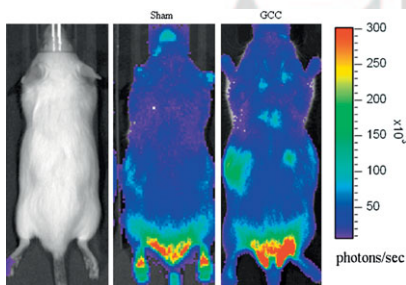
- Names of all authors present and spelled correctly
- Titles of authors correct (Prof. or Dr. only: please note, Prof. Dr. is not used in the journals)
- Addresses and postcodes correct
- E-mail address of corresponding author correct (current email address)
- Funding bodies included and grant numbers accurate
- Title of article OK
- All figures included. Resolution OK (If not, you can provide new figures with your corrections)
- Equations correct (symbols and sub/superscripts)

This list is for your convenience. There is no need to return it with your corrections. If you have any queries, please contact the editorial office at the email address above.

mabi.201000498C

Full Paper

A novel glutaraldehyde-cross-linked casein protein (GCC) conduit is developed. NF- $\kappa$ B-dependent bioluminescence in living mice is used to monitor the immune response caused by the implanted GCC conduit. Subsequently, this new protein-based biodegradable conduit is submitted to mechanical, cytotoxic, morphological, and biological tests. Results show that the conduit has properties of great interest towards the repair of regenerating nerve tissues.



**Biodegradable  
Glutaraldehyde-crosslinked  
Casein Conduit Promotes  
Regeneration after Peripheral  
Nerve Injury in Adult Rats**

W. Wang, J. -H. Lin, C. -C. Tsai,  
H. -C. Chuang, C. -Y. Ho, C. -H. Yao,  
Y. -S. Chen\*

*Macromol. Biosci.* **2011**, *11*, 000–000

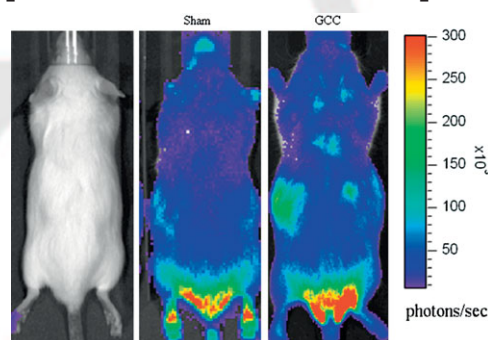


Early View Publication; these are  
NOT the final page numbers,  
use DOI for citation !!

# Biodegradable Glutaraldehyde-crosslinked Casein Conduit Promotes Regeneration after Peripheral Nerve Injury in Adult Rats

Walter Wang, Jia-Horng Lin, Chin-Chuan Tsai, Hao-Che Chuang, Chien-Yi Ho,<sup>a</sup> Chun-Hsu Yao,<sup>a</sup> Yueh-Sheng Chen<sup>\*a</sup>

In this study, GCC protein was used for the first time to construct a biodegradable conduit for peripheral nerve repair. The GCC was highly stable with a sufficiently high level of mechanical properties and it was non-toxic and non-apoptotic which could maintain the survival and outgrowth of Schwann cells. Noninvasive bioluminescence imaging accompanied with histochemical assessment showed the GCC was highly biocompatible after subcutaneous implantation in transgenic mice. Electrophysiology, labeling of calcitonin gene-related peptide in the lumbar spinal cord and histology analysis also showed a rapid morphological and functional recovery for disrupted rat sciatic nerves repaired with the GCC conduits. Therefore, we conclude that the GCC can offer great nerve regeneration characteristics and can be a promising material for the successful repair of peripheral nerve defects.



W. Wang, C.-H. Yao, Y.-S. Chen, PhD  
Laboratory of Biomaterials, School of Chinese Medicine, China Medical University, Taichung, Taiwan  
Fax: 886-4-22032295; E-mail: yuehsc@mail.cmu.edu.tw

J.-H. Lin  
Laboratory of Fiber Application and Manufacturing, Graduated Institute of Textile Engineering, Feng Chia University, Taichung Taiwan

C.-C. Tsai  
School of Chinese Medicine for Post-Baccalaureate, I-Shou University, Kaohsiung, Taiwan

C.-C. Tsai  
Chinese Medicine Department, E-DA Hospital, Kaohsiung, Taiwan

H.-C. Chuang  
Department of Neurosurgery, China Medical University Hospital, China Medical University, Taichung, Taiwan

C.-Y. Ho  
Department of Family Medicine, China Medical University Hospital, China Medical University, Taichung, Taiwan

C.-H. Yao  
Department of Biomedical Imaging and Radiological Science, China Medical University, Taichung, Taiwan

<sup>a</sup> Those authors contributed equally to this work.

## Introduction

For improving peripheral nerve regeneration, the development of biomaterials to make nerve bridge conduits has attracted considerable attention in recent years. A nerve bridge technique is the introduction of both ends of the injured nerve stumps into a tubular chamber, which can offer the advantages of aiding guidance of growing fibers along appropriate paths by mechanical orientation and confinement, and enhancing the precision of stump approximation. Several synthetic materials, either non-degradable<sup>[1–3]</sup> or biodegradable,<sup>[4–6]</sup> have been used as a nerve conduit. The main objection for using non-degradable conduits is that they remain in situ as foreign bodies after the nerve has regenerated and may require a second surgery to remove the conduits, causing possible damage to the nerve.<sup>[7,8]</sup> Therefore, biodegradable conduits seem a more promising alternative to reconstruct nerve gaps. An ideal biodegradable conduit should maintain its structural integrity, permitting cell infiltration and subsequent tissue growth during the regenerative processes.<sup>[9]</sup> Nowadays,

several biodegradable nerve conduits have been approved by the Food and Drug Administration (FDA) for nerve repair in clinics, such as SaluBridge<sup>®</sup> (poly(vinyl alcohol)), Neurotube<sup>®</sup> (poly(glycolic acid)), and NeuraGen<sup>®</sup> (collagen). In the present study, we developed a novel protein-based biodegradable conduit for nerve repair. For this purpose, casein, a predominant phosphoprotein accounting for nearly 80% of proteins in cow milk was crosslinked by glutaraldehyde.<sup>[10,11]</sup> To understand physical characteristics of the glutaraldehyde-crosslinked casein (GCC) conduits, we evaluated their mechanical function, water uptake ratio, and hydrophilicity. Cytotoxic testing and terminal deoxynucleotidyl transferase dUTP nick end labeling (TUNEL) of the conduits were determined by using the Schwann cell line, which has been extensively adopted to study neural cell differentiation,<sup>[12–14]</sup> to study cell viability upon exposure to the substances released from soaked GCC conduits. The inflammatory response is a key component in the biocompatibility of biomaterials. Among the factors that control the development of inflammation is a critical molecule nuclear factor kappa- $\kappa$ B (NF- $\kappa$ B).<sup>[15,16]</sup> Therefore, NF- $\kappa$ B-dependent luminescent signal in transgenic mice carrying the luciferase genes was used as the guide to assess the host-GCC interaction. In addition, it has been reported that regeneration process may be directly impaired in regenerative microenvironment caused by deficits in action of vasoactive neuropeptides such as calcitonin gene-related peptide (CGRP).<sup>[17,18]</sup> Since the CGRP expression has an impact on nature of peripheral nerve regeneration<sup>[19]</sup> that we tested the possibility that constructed GCC conduits promote axonal regeneration and functional restoration by examining the CGRP in the lumbar spinal cord by immunohistochemistry, and correlating morphometric and electrophysiological data in 1 cm Sprague-Dawley (SD) rat sciatic nerve defect.

## Experimental Section

### Fabrication of GCC Conduits

A 20% (w/w) solution of casein (Sigma #C5890, Saint Louis, MO) in 0.2 M Na<sub>2</sub>HPO<sub>4</sub> buffer was prepared by magnetic stirring. A silicone rubber tube (1.96 mm OD; Helix Medical, Inc., Carpinteria, CA) was used as a mandrel vertically dipped into the casein solution at a constant speed where it remained for 2 min. The mandrel was then withdrawn slowly and allowed to stand for 25 min for air-drying. The mandrel was rotated horizontally consistently to reduce variations in the wall thickness along the axis of the tube. Four coating steps were used and the casein-coated mandrel was then immersed in 0.1% (w/w) solution of glutaraldehyde (Sigma #G5882, Saint Louis, MO) for 30 min for cross-linking. The coated mandrel was rinsed twice with distilled water, dehydrated for 10 min with 95% of ethanol, and air-drying for 1 week. The GCCs were slipped off the silicone rubber mandrel and cut to 12 mm length. To allow fixation of the nerve tissue to the conduit, two small holes were

drilled at both ends of the GCCs. Finally, the GCCs were sterilized with 25 kGy of  $\gamma$ -ray for subsequent implantation.

### Cross-linking Degree of GCC Conduits

Ninhydrin assay was used to evaluate the cross-linking degree of GCC conduits. Ninhydrin (2,2-dihydroxy-1,3-indanedione) was used to determine the amount of amino groups of each test sample. The test GCC conduits were heated with a ninhydrin solution for 20 min. After heating with ninhydrin, the optical absorbance of the solution was recorded using a spectrophotometer (Model Genesys<sup>TM</sup> 10, Spectronic Unicam, New York, NY) at 570 nm (wavelength of the blue-purple color) using casein at various known concentrations as standard. The amount of free amino groups in the residual casein, after heating with ninhydrin, is proportional to the optical absorbance of the solution. The cross-linking degree of GCC conduits was then determined.

### Macroscopic Observation of GCC Conduits

To examine the morphology of the GCC explants with scanning electron microscopy (SEM), the samples were gold-coated using a Hitachi E-1010 Ion Sputter and micrographs were obtained using a Hitachi S3000N scanning electron microscope at an accelerating voltage of 5 kV.

### Mechanical Function of GCC Samples

The mechanical properties of GCC were determined in a dry condition. All test samples were preconditioned at 50% humidity and 23 °C for 48 h. The maximum tensile strength was determined by the universal testing machines (AG-IS, Shimadzu Co., Japan). All test samples, cut into dumbbell shape (Figure 1), were pulled at an extension rate of 0.6 mm · min<sup>-1</sup>. Measurements were made five times for each sample and averages were reported.

### Water Contact Angle Analysis of GCC Samples

Drops of distilled water were placed on the GCC films and contact angles were measured using a static contact angle meter (CA-D, Kyowa, Japan). An auto pipette was employed with the meter to ensure that the volume of the distilled water droplet was the same (20  $\mu$ L) for each specimen.

### Water Uptake Ratio of GCC Conduits

The weight equilibrium water uptake ratio was experimentally determined using the following equation:

$$\text{water uptake ratio} = (W_t - W_0) / W_0$$

where  $W_t$  is the weight of the swollen test sample and  $W_0$  is the weight of the dried test sample. The measuring of water uptake ratio in each step is carefully conducted six times at 0.5, 1, 3, 6, 12, 24, 48, 60, 72 and 84 h after GCC conduits were soaked in 10 ml of de-ionized water of pH 7.4 at room temperature. In addition, the luminal areas of the soaked GCC conduits at 24, 48, and 72 h were measured.

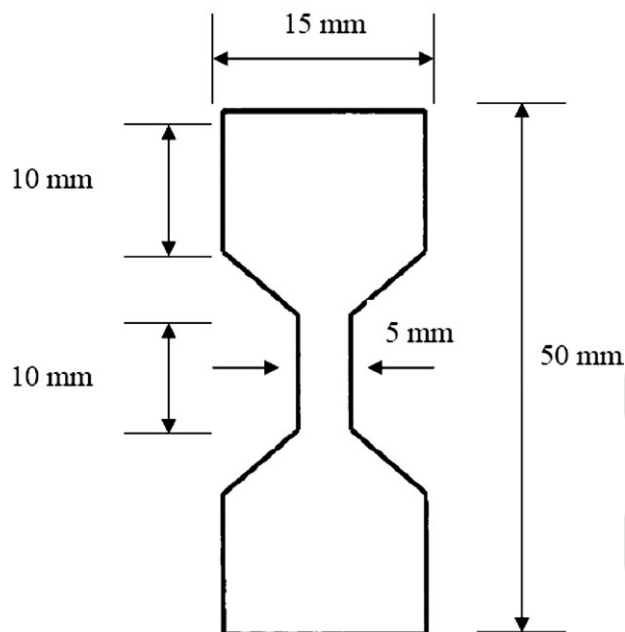


Figure 1. Schematic drawing of the dumbbell-shaped sample used in the mechanical testing (not to scale).

paraformaldehyde for 30 min and then permeabilized with 0.1% Triton X-100/PBS for 30 min at room temperature. After washing with PBS, TUNEL assay was performed according to the manufacturer's instructions (Roche Diagnostics, Mannheim, Germany). Cells were incubated in TUNEL reaction buffer in a 37 °C humidified chamber for 1 h in the dark, then rinsed twice with PBS and incubated with DAPI (1 mg · ml<sup>-1</sup>) at 37 °C for 10 min, stained cells were visualized using a fluorescence microscope (Olympus DP70/U-RFLT50, Olympus Optical Co., Ltd., Japan). TUNEL-positive cells were counted as apoptotic cells.

### Tissue Reactions to GCC Conduits

Prior to the beginning of the in vivo testing, the protocol was approved by the ethical committee for animal experiments of the China Medical University, Taichung, Taiwan. Transgenic mice, carrying the luciferase gene driven by NF-κB-responsive elements, were constructed as described previously.<sup>[15,16]</sup> All transgenic mice were crossed with wild-type F1 mice to yield NF-κB-luc heterozygous mice with the FVB genetic background. For insertion of the GCC implant, transgenic mice were anesthetized with 0.12 g ketamine/kg body weight and one incision (3 mm in length) on the back was made. The GCC conduit was then implanted subcutaneously into the incision and the skin was closed with silk sutures. A total of 6 transgenic mice were randomly divided into two groups of three mice: (1) sham, the incision was made and nothing was implanted and (2) GCC, the incision was made and the GCC conduit was implanted. The mice were imaged for the luciferase activity at various time points: 1 d, 3 d, 7 d, and 28 d and subsequently sacrificed for histochemical staining. For in vivo imaging, mice were anesthetized with isoflurane and injected intraperitoneally with 150 mg luciferin/kg body weight. Five minutes later, mice were placed facing down in the chamber and imaged for 5 min with the camera set at the highest sensitivity by IVIS Imaging System<sup>®</sup> 200 Series (Xenogen, Hopkinton, MA). Photons emitted from tissues were quantified using Living Image<sup>®</sup> software (Xenogen, Hopkinton, MA). Signal intensity was quantified as the sum of all detected photon counts per second within the region of interest after subtracting the background luminescence and presented as photons · sec<sup>-1</sup> · cm<sup>-2</sup> · sr<sup>-1</sup> (sr = steradian). For histochemical staining, the GCC implants were retrieved and fixed in 10% formalin for 2 d. Tissue was rinsed in saline and dehydrated in a series of graded ethanol (50%, 70%, and 95%) for 30 min each. Samples were then embedded in paraffin and cut into thin 12-μm sections. For histomorphometric evaluation, sections were stained with hematoxylin and eosin. The tissue reactions to the implants in the subcutaneous tissue were evaluated for uniformity and thickness of the foreign body capsule as well as the inflammation responses, such as distribution of inflammatory cells and phagocytising reaction under optical microscopy (Olympus IX70, Olympus Optical Co., Ltd., Japan).

### GCC Conduits Implantation

Thirty adult SD rats underwent placement of GCC conduits, which were removed upon sacrifice at various time points: 2 weeks, 5 weeks, and 8 weeks. At each implantation time, 10 rats were operated on. The animals were anesthetized with an inhalational

1 **Q1** authors, how did you obtain DI water with a pH of 7.4  
2 (should be either pH 7.0 or a little less due to CO<sub>2</sub> from the  
3 atmosphere!) ?■

### Cytotoxicity and Apoptosis of GCC Digestion By-products

4 The indirect cytotoxicity was conducted in adaptation from the  
5 ISO10993-12 standard test method.<sup>[20]</sup> GCC conduits of 6 cm<sup>2</sup> were  
6 washed twice with sterilized 1 × PBS and dried in a laminar flow.  
7 GCC digestion by-products were prepared by incubating the  
8 conduit in 1 ml of serum free Dulbecco's Modified Eagle's Medium  
9 (DMEM) at 37 °C for 24 h in an incubator with 75% humidity  
10 containing 5% CO<sub>2</sub>. RSC96 Schwann cells were seeded at  
11 1 × 10<sup>4</sup> cells/well in a 96-well tissue-culture polystyrene plate  
12 (TCPP; Corning, USA) at 37 °C for 24 h in an incubator with 75%  
13 humidity containing 5% CO<sub>2</sub>. After that, the culture medium was  
14 removed and replaced with the GCC digestion by-products (200 μL/  
15 well). After 24 h of cell incubation with the GCC digestion by-  
16 products, the solution was removed, replaced with 110 μL/well of  
17 5 mg · ml<sup>-1</sup> of 3-(4,5-Dimethylthiazol-2-yl)-2,5-diphenyltetrazo-  
18 liumbromid (MTT) solution in 1 × PBS and further incubated in  
19 an incubator at 37 °C for 4 h. Then, the MTT solution was removed  
20 and replaced with 50 μL of dimethylsulfoxide (DMSO) to dissolve  
21 the formazan. The color intensity was measured using a microplate  
22 reader (ELx800TM, Bio-Tek Instrument, Inc., Winooski, VT, USA)  
23 at the absorbance of 550 nm. Data were then expressed as a  
24 percent of control level of the optical density within an individual  
25 experiment.

26 Apoptotic cell death was also confirmed in the present study.  
27 After treating with the GCC digestion by-products for 48 h, the  
28 Schwann cells were washed with PBS twice, fixed in 2%

1 anesthetic technique (AErrane<sup>®</sup>, Baxter, USA). Following the skin  
2 incision, fascia and muscle groups were separated using blunt  
3 dissection, and the right sciatic nerve was severed into proximal  
4 and distal segments. The proximal stump was then secured with a  
5 single 9-0 nylon suture through the epineurium and the outer wall  
6 of the GCC conduits. The distal stump was secured similarly into the  
7 other end of the chamber. Both the proximal and distal stumps  
8 were secured to a depth of 1 mm into the chamber, leaving a 10-mm  
9 gap between the stumps. The muscle layer was re-approximated  
10 with 4-0 chromic gut sutures, and the skin was closed with 2-0 silk  
11 sutures. All animals were housed in temperature (22 °C) and  
12 humidity (45%) controlled rooms with 12 h light cycles, and they  
13 had access to food and water ad libitum.

### Electrophysiological Techniques

14 The animals were re-anaesthetized and their sciatic nerve exposed.  
15 The stimulating cathode was a stainless-steel monopolar needle,  
16 which was placed directly on the sciatic nerve trunk, 5-mm  
17 proximal to the transection site. The anode was another stainless-  
18 steel monopolar needle placed 3-mm proximally to the cathode.  
19 Amplitude, latency, duration, and nerve conductive velocity (NCV)  
20 of the evoked muscle action potentials (MAP) were recorded from  
21 gastrocnemius muscles with micro-needle electrodes linked to a  
22 computer system (Biopac Systems, Inc., USA). The latency was  
23 measured from stimulus to the takeoff of the first negative  
24 deflection and the amplitude from the baseline to the maximal  
25 negative peak. The NCV was carried out by placing the recording  
26 electrodes in the gastrocnemius muscles and stimulating the  
27 sciatic nerve proximally and distally to the nerve conduit and  
28 calculated by dividing the distance between the stimulating sites  
29 by the difference in latency time. All data are expressed as  
30 mean ± standard deviation. Statistical comparisons between  
31 groups were made by the one-way analysis of variance.

### Histological Processing

32 Immediately after the recording of muscle action potential, all of  
33 the rats were perfused transcardially with 150 ml normal saline  
34 followed by 300 ml 4% paraformaldehyde in 0.1 M phosphate  
35 buffer, pH 7.4. After perfusion, the L4 spinal cord was quickly  
36 removed and post-fixed in the same fixative for 3–4 h. Tissue  
37 samples were placed overnight in 30% sucrose for cryoprotection at  
38 4 °C, followed by embedding in optimal cutting temperature  
39 solution. Samples were kept at –20 °C until preparation of  
40 18 μm sections was performed using a cryostat, with samples  
41 placed upon poly-L-lysine-coated slide. Immunohistochemistry of  
42 frozen sections was carried out using a two-step protocol according  
43 to the manufacturer's instructions (Novolink Polymer Detection  
44 System, Novocastra). Briefly, endogenous peroxidase activity in  
45 frozen sections was inactivated with incubation of the slides in  
46 0.3% H<sub>2</sub>O<sub>2</sub>, and nonspecific binding sites were blocked with Protein  
47 Block (RE7102; Novocastra). After serial incubation with rabbit  
48 anti-CGRP polyclonal antibody 1:1000 (Calbiochem, Germany),  
49 Post Primary Block (RE7111; Novocastra), and secondary antibody  
50 (Novolink Polymer RE7112), the sections were developed in  
51 diaminobenzidine solution under a microscope and counterstained  
52 with hematoxylin. Sciatic nerve sections were taken from the

1 middle regions of the regenerated nerve in the chamber. After the  
2 fixation, the nerve tissue was post-fixed in 0.5% osmium tetroxide,  
3 dehydrated, and embedded in spurs. The tissue was then cut to 5-  
4 μm thickness by using a microtome with a dry glass knife, stained  
5 with toluidine blue.

### Image Analysis

6 All tissue samples were observed under optical microscopy. CGRP-  
7 immunoreactivity (IR) in dorsal and ventral horns in the lumbar  
8 spinal cord was detected by immunohistochemistry as described  
9 previously.<sup>[21]</sup> The immuno-products were confirmed positive-  
10 labeled if their density level was over five times of background  
11 levels. Under a 100× magnification, the ratio of area occupied by  
12 positive CGRP-IR in the dorsal horn and CGRP-expressing cells in the  
13 ventral horn following neurorrhaphy relative to the lumbar spinal  
14 cord bilaterally was measured using an image analyzer system  
15 (Image-Pro Lite, Media Cybernetics, USA) coupled to the micro-  
16 scope. Statistical comparisons between groups at different time  
17 points post-surgery were made by the one-way analysis of  
18 variance. Student's t-test was used to compare the bilateral  
19 CGRP-IR differences at the same time point.

20 As counting the myelinated axons, at least 30 to 50% of the  
21 sciatic nerve section area randomly selected from each nerve  
22 specimen at a magnification of 400× was observed. The axon  
23 counts were extrapolated by using the area algorithm to estimate  
24 the total number of axons for each nerve. Axon density was then  
25 obtained by dividing the axon counts by the total nerve areas.  
26 Statistical comparisons between groups were made by the one-  
27 way analysis of variance.

## Results and Discussion

### Macroscopic Observation of GCC Conduits

28 GCC conduits were brownish in appearance caused by the  
29 reaction between glutaraldehyde and amino acids or  
30 proteins. Figure 2 shows that the GCC conduit was  
31 concentric and round with a smooth inner lumen and  
32 outer wall surface.

### Physical Characteristics of GCC Conduits

33 The cross-linking index of GCC conduits, expressed as a  
34 percentage of free amino groups lost during cross-linking,  
35 was 77.1 ± 0.7%. It means that a 1.0 wt.-% glutaraldehyde  
36 solution (30 min) was sufficient to cross-link about 77.1% of  
37 the amino groups. The maximum tensile strength and the  
38 water contact angle of GCC conduits were 44.2 ± 4.7 MPa  
39 and 58.4 ± 6.9 degree. Compared to the biodegradable  
40 materials reported in the literature (Table 1), the GCC  
41 had a relatively larger maximum tensile strength at  
42 44.2 ± 4.7 MPa which should have sufficient tensile  
43 strength to be utilized as a nerve graft when compared  
44 to the tensile strength of fresh rat sciatic nerve

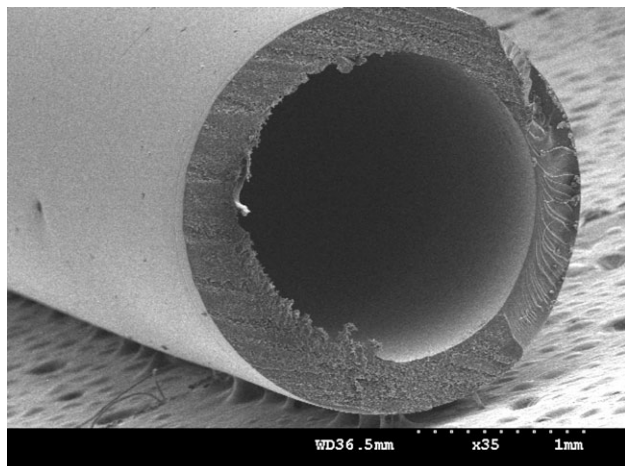


Figure 2. SEM micrograph of the GCC conduit.

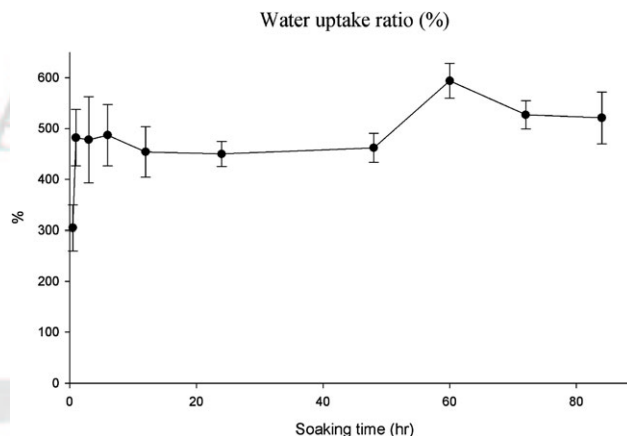


Figure 3. Time effect on the water uptake ratio of soaked GCC conduits.

(2.72 ± 0.97 MPa) reported by Borschel et al.<sup>[32]</sup> In addition, the water contact angle of the GCC was 58.4 ± 6.9 degree which was hydrophilic that should be conducive to cell adhesion and growth. Figure 3 represents the water uptake ratios of the soaked GCC conduits. In the first 6 h, the weight uptake of the GCC conduits increased markedly. A tendency for attenuated water uptake was observed which was almost at a plateau when the soaking period exceeded 6 h. Similarly, the luminal areas of the GCC conduits were increased dramatically (Table 2). However, all of the GCC conduits still maintained the lumens and wall integrity even after 80 h of soaking, indicating that the GCC matrix provided a framework with high mechanical strength.

### Cytotoxicity and Apoptosis of GCC Conduits

Spindle-shaped cellular morphology of Schwann cells cultured on the culture plate was viable and there was

no sign of infection. The color of DMEM with the digestion products of the GCC conduits after 24 h became yellowish. Treatment with the GCC digestion by-products did not induce apoptotic cell death since only very few TUNEL positive cells were seen, suggesting that the DNA fragmentation did not occur in these Schwann cells (Figure 4A). This result was supported by the cytotoxic test that the optical density of the Schwann cells was not significantly different as compared to that of the controls after exposing to the GCC digestion by-products (Figure 4B), indicating that these conduits would not induce cytotoxic effects to the cultured cells.

### Tissue Reactions to GCC Conduits

No intense foreign-body reactions or necrosis of tissues were seen for any of the rats in the postoperative period. The GCC implant was implanted subcutaneously on the back of

Table 1. Maximum tensile strength and water contact angle of nerve bridging materials reported in the literature.

Materials	Maximum tensile strength [MPa]	Water contact angle [°]
(1) collagen-chitosan <sup>[22]</sup>	0.2482 to 0.3612	N/A
(2) collagen crosslinked by EDC/NHS <sup>[23]</sup>	77.9 to 92.5	44.1 to 74.9
(3) collagen-chitosan-polyurethane <sup>[24]</sup>	9.38	N/A
(4) poly( $\epsilon$ -caprolactone) <sup>[25]</sup>	10.73 to 16.3	36.7 to 80.03
(5) chitosan <sup>[26]</sup>	0.64	N/A
(6) poly[(D,L-lactide)-( $\epsilon$ -caprolactone)] <sup>[27]</sup>	13	N/A
(7) collagen-glycosaminoglycan <sup>[28]</sup>	0.002	N/A
(8) poly[(L-lactic acid)-co-poly( $\epsilon$ -caprolactone)]/collagen <sup>[29]</sup>	4.61	57
(9) poly( $\epsilon$ -caprolactone)/gelatin <sup>[30]</sup>	0.8	32
(10) poly(ethylene glycol)-graft- poly(D,L-lactic acid) <sup>[31]</sup>	N/A	50.4

Table 2. Luminal areas of the soaked GCC conduits.

Soaking time [hr]	0	24	48	72
Luminal area [mm <sup>2</sup> ]	66.0 ± 3.8	125.9 ± 8.6	166.6 ± 7.5	187.6 ± 7.2

the mice and the NF- $\kappa$ B-driven bioluminescent signals were monitored by luminescent imaging on the indicated periods (Figure 5A). As a result, the luminescent signal in the implanted region was initially increased and dramatically decreased (Figure 5B). NF- $\kappa$ B activity reached a maximal activation at 3 d where a strong and specific *in vivo* bioluminescence around the implantation site was observed. In consistent with the bioluminescent signals, an acute inflammatory response was characterized by a rapid accumulation of cells resembling lymphocytes and macrophages at the site between GCCs and their surrounding tissue at 1 d post-implantation (Figure 6A). GCCs still persisted maintaining their lumens and wall integrity at this time point. At 3 d, a delicate fibrous tissue capsule with dispersing neocapillaries was present surrounding the whole implant. Inflammation responses were still obvious with abundant inflammatory cells (Figure 6B). Phagocytosing reaction became obvious at the interfaces between the GCC materials and tissues after 7 d of implantation (Figure 6C). At the time points of 28 d, fibrous tissue

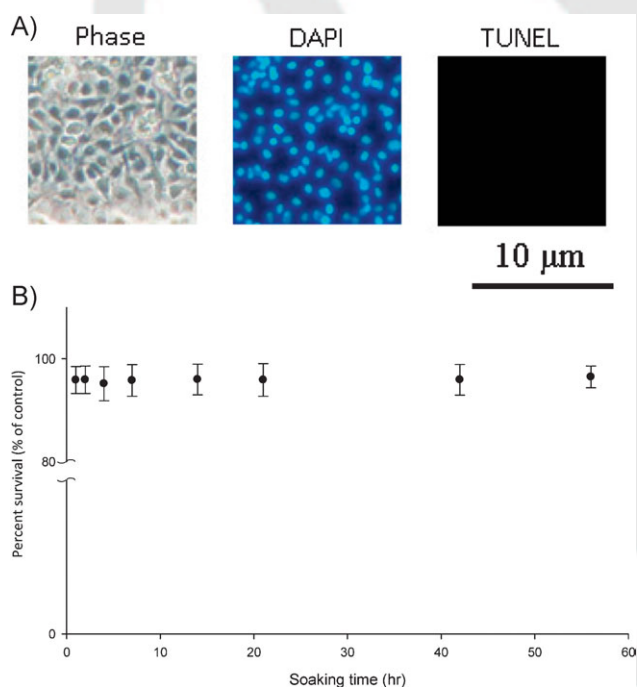


Figure 4. Induction of apoptosis and cytotoxicity by soaking solution of GCC conduits. (A) Nuclei of Schwann cells were characterized by DAPI and TUNEL assay and investigated under a fluorescence microscope. (B) Quantification of cytotoxic test of soaking solutions of GCC conduits relative to the controls on Schwann cells. Values are mean  $\pm$  standard error.

capsules became thicker with a compact structure along with active neovascularization. Up to this time, inflammatory reaction continued with macrophages digesting the fragmented GCC materials (Figure 6D).

### Electrophysiological Measurements

MAPs were recorded at postoperative intervals of 2, 5, and 8 weeks. All of the electrophysiological indexes, including amplitude, latency, duration, and NCV of the regenerated

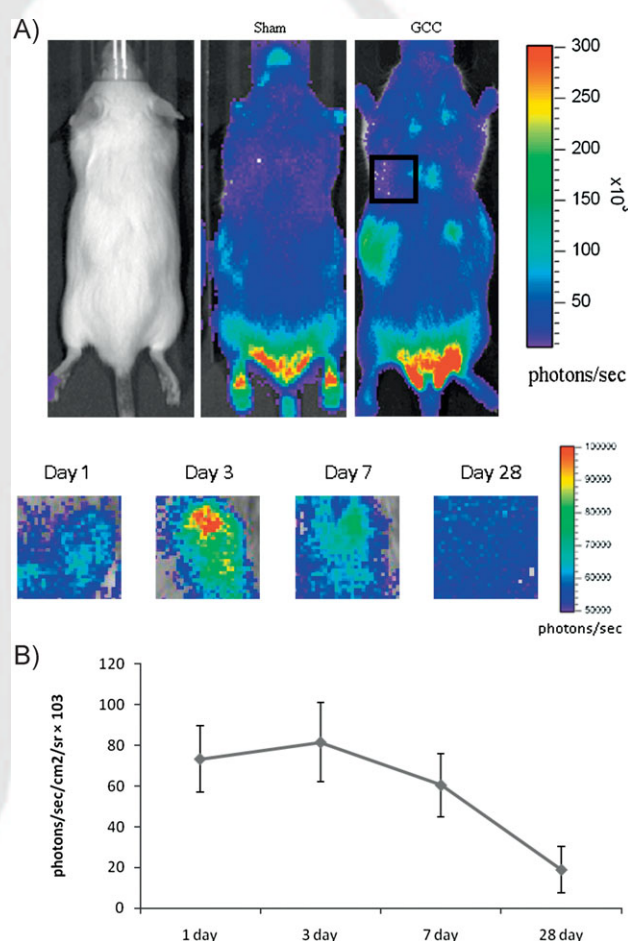


Figure 5. NF- $\kappa$ B-dependent bioluminescence in living mice implanted with GCC conduits. (A) Diagrams show the bioluminescent signal within a radius of 2.5 mm of implanted region (boxed area). The color overlay on the image represents the photons  $\cdot$  s<sup>-1</sup> emitted from the animal, as indicated by the color scales. (B) Quantification of photon emission within the implanted region. Values are mean  $\pm$  standard error of three mice.



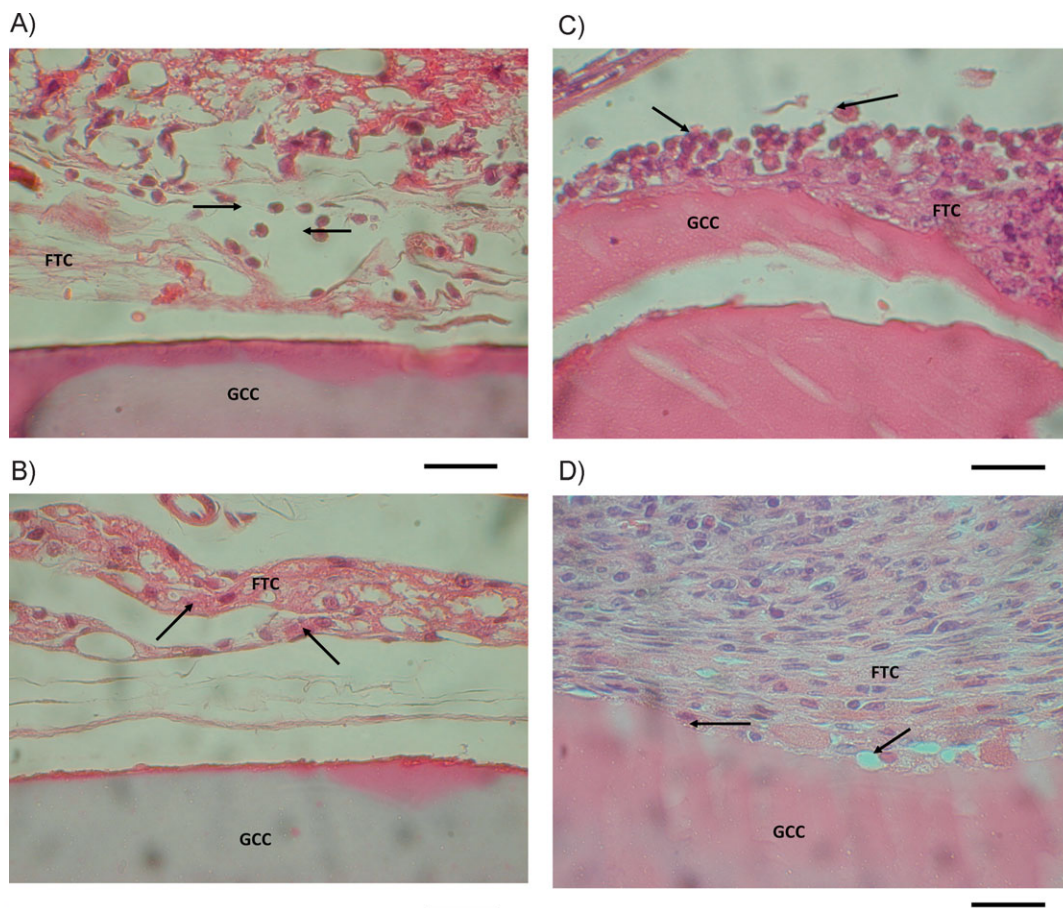


Figure 6. Micrograph of interface area between the host and GCC conduits implanted for (A) 1 d, (B) 3 d, (C) 7 d, and (D) 28 d. Note a rapid accumulation of inflammatory cells (arrows) phagocytising the disintegrated GCC materials. Fibrous tissue capsules (FTC) were thick with a compact structure at 28 d after implantation. Scale bars: 100  $\mu\text{m}$ .

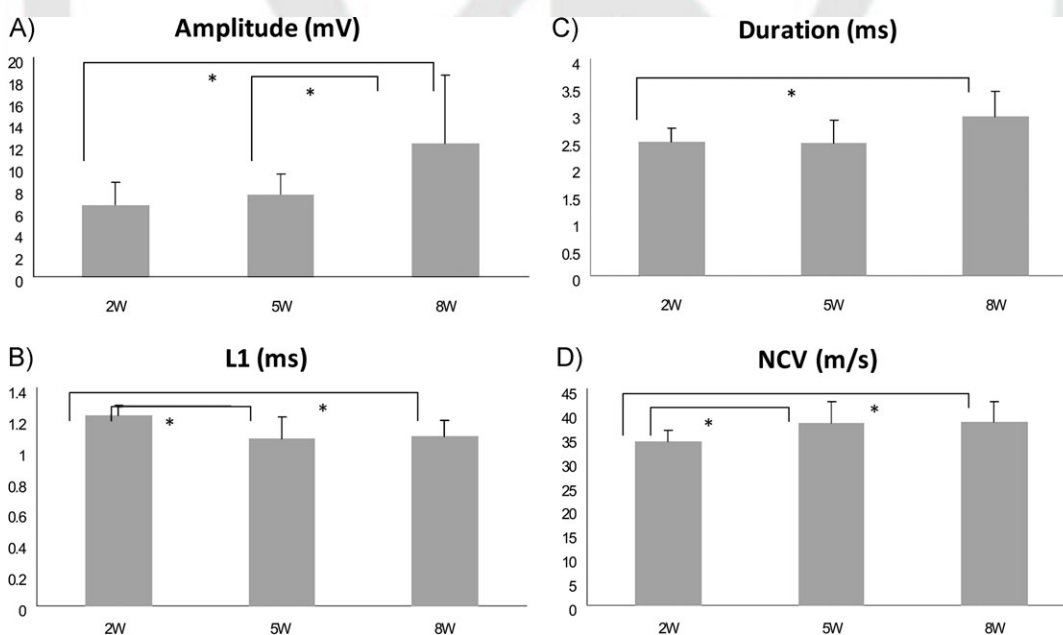


Figure 7. Analysis of the evoked muscle action potentials, including (A) peak amplitude, (B) latency, and (C) NCV. \* $P < 0.05$ , significant difference from other examined time points.

1 nerves were improved as a function of the experimental  
2 period (Figure 7A-7D). Specifically, the regenerated nerves  
3 at 8 weeks postoperatively had a significantly shorter  
4 latency and larger duration, amplitude and NCV as  
5 compared to those at 2 and 5 weeks of recovery.

### CGRP-IR in the Spinal Cord

6 Immunohistochemical staining showed that CGRP-labeled  
7 fibers were noted in the area of lamina III-V (Figure 8).  
8 Lamina I-II regions in the dorsal horn of the lumbar spinal  
9 cord bilaterally were strongly CGRP-immunolabeled on  
10 week 2, and then notably decreased on weeks 5 to 8  
11 (Figure 9A-9B). In addition, CGRP-expressing cells in the  
12 ventral horns of the lumbar spinal cord bilaterally  
13 displayed the typical morphological characteristics of  
14 motoneurons (Figure 9C-9D). Specifically, the ratio of area  
15 occupied by positive CGRP-IR ipsilateral to the injury was  
16 significantly decreased on week 8 compared to that on  
17 week 2 post-surgery (Figure 10A-10B). Similarly, the CGRP-  
18 expressing cell numbers in the ventral horns peaked on

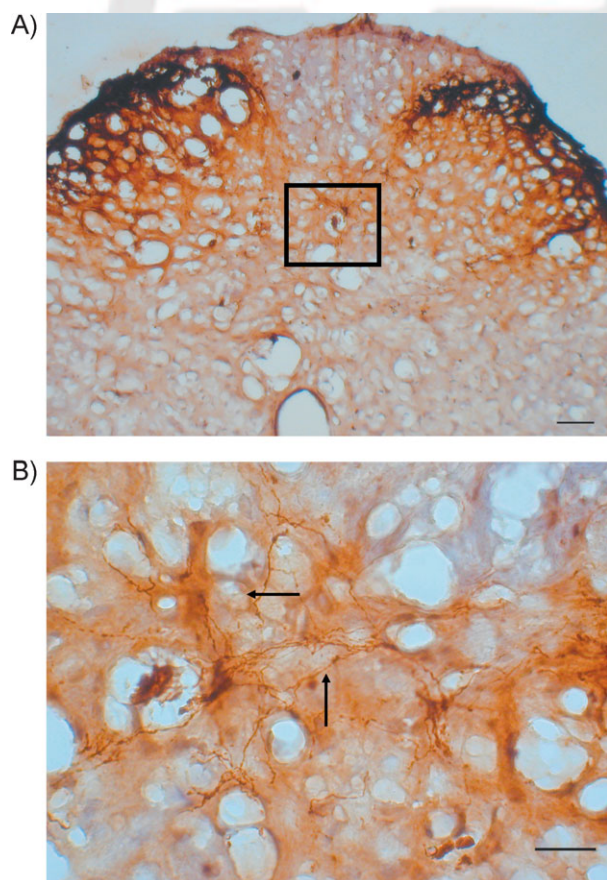


Figure 8. CGRP-IR in the lumbar spinal cord after injury. (A) The area of lamina III-V examined for CGRP-labeled fibers (arrows). Shown in (B) is the higher magnification of the boxed area in (A). Scale bars: 100  $\mu\text{m}$  for panel A, 25  $\mu\text{m}$  for panel B.

week 2 post-injury, and dramatically declined from weeks 5  
to 8 (Figure 10C-10D). It was noted that the CGRP-IR area  
ratios and the CGRP-expressing cell numbers ipsilateral to  
the injury were all relatively larger than those from  
contralateral IR at the three different time point post-  
surgery (Figure 11A-11B). Specifically, the bilateral differ-  
ences in CGRP-IR area ratios on week 2 and CGRP-expressing  
cell numbers on weeks 2 and 5 differed significantly. These  
results indicated that CGRP expression differed depending  
upon the location in the lumbar spinal cord and the  
recovery stage of regenerating sciatic nerve in the GCC  
conduit.

### Sciatic Nerve Regeneration

Throughout the 8 weeks of experimental period, no nerve  
dislocation out of the GCC conduits was seen for any of the  
rats. Brownish fibrous tissue encapsulation was noted,  
covering all over the GCC conduits. After trimming the  
fibrous tissue, cutting the wall of the tube, the regenerated  
nerve was exposed and then retrieved. Observing the  
muscle tissue surrounding the conduit, no obvious inflam-  
mation or adhesion was found. Overall gross examination  
of the GCC conduits at the three observation time points  
all revealed 100% of nerve formation in the tubes.

At 2 weeks post-implantation, swelling or deformation  
of the GCCs was not seen. Regenerated nerves in the GCCs  
were still immature composed of fibrin matrices, which  
were populated by Schwann cells and blood vessels  
(Figure 12A). At this stage, it is difficult to discriminate  
between the endoneurial areas and their surrounding  
fibrous tissues.

At 5 weeks, the GCCs featured a partially fenestrated  
outer layer; however, they still remained circular with a  
round lumen. Up to this time, the regenerated nerves  
became more mature, displaying a structure with a  
symmetric epineurium, surrounding a cellular and vascularized  
endoneurium in which numerous myelinated axons  
had been seen (Figure 12B).

At 8 weeks, fragmentation of the GCCs continued but  
their architecture still remained. As seen at 5 weeks of  
regeneration, the nerves at this stage had a mature  
structure with a large number of myelinated axons  
interposed in the endoneurium with rich neovasculariza-  
tion (Figure 12C).

By comparison, the nerve maturity and the spatial  
temporal progression of cellular activity within the GCC  
conduits are similar to those seen in the silicone rubber  
conduits.<sup>[33]</sup>

### Morphometric Measurements

As aforementioned results, nerve features in the GCC  
conduits at 2 weeks of implantation were too immature to

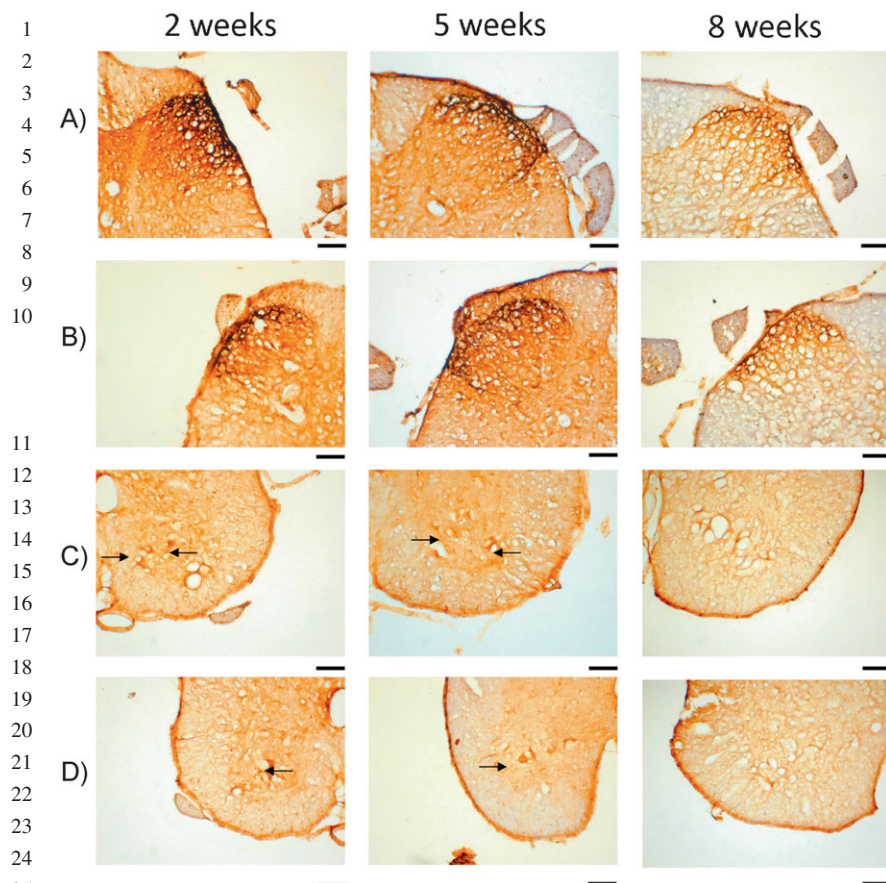


Figure 9. CGRP-IR in the (A) dorsal horn ipsilateral to the injury, (B) dorsal horn contralateral to the injury. CGRP-expressing cells (arrows) in the (C) ventral horn ipsilateral to the injury, (D) ventral horn contralateral to the injury. Scale bars: 100  $\mu$ m

be included in comparisons of their morphometric measurements. By comparison, morphometric studies revealed available data in regenerated nerves in both the tube groups after 5 and 8 weeks of implantation. No significant difference was seen between the mean values of their myelinated axon number, axon area, axon density, and total nerve area (Figure 13A-13D).

### General Discussion

Peripheral nerve injuries are very common in clinical practice. Nowadays, autologous nerve grafting is the most commonly used technique to reconstruct the peripheral nerve defect. However, grafting has a number of inevitable disadvantages including morbidity at the donor site and limited supply of donor nerves.<sup>[34,35]</sup> Though nerve allografts may be used to overcome these problems, few successes were achieved due to the immunological rejection.<sup>[36,37]</sup> Therefore, the use of an artificial guide for reconstruction of nerve gaps can be seen as an alternative. In recent years, enormous efforts in clinical and experimental investigations have been made to seek

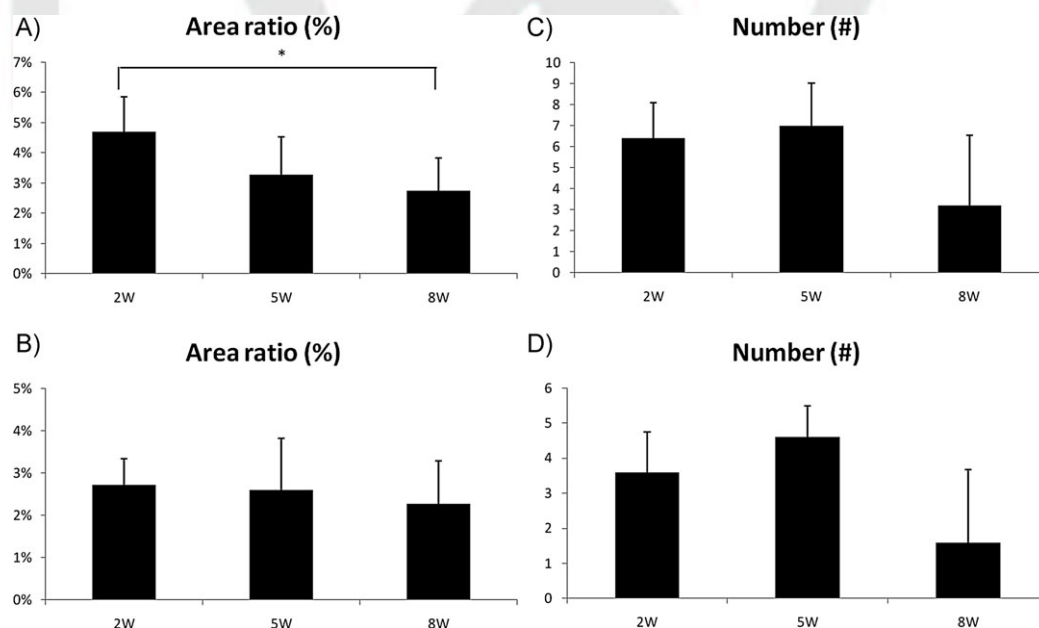
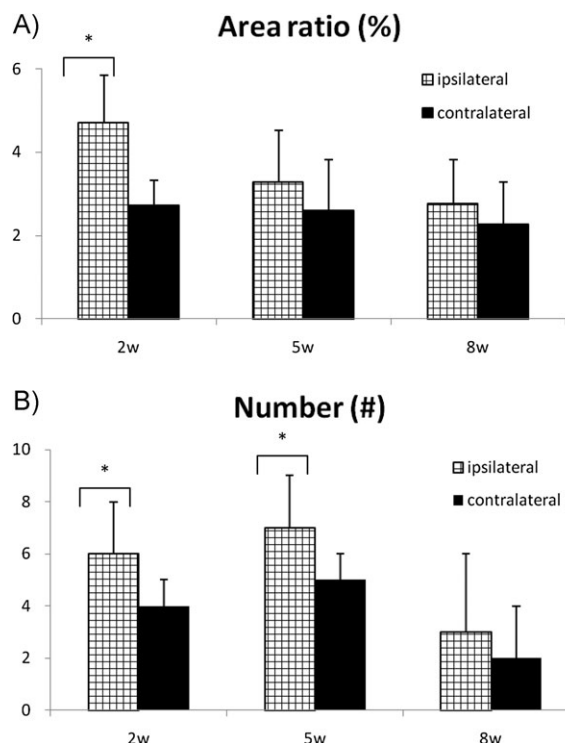


Figure 10. Comparisons of CGRP-IR area ratios at different time points post-surgery in the (A) dorsal horns ipsilateral to the injury (B) dorsal horn contralateral to the injury and CGRP-expressing cell numbers in the (C) ventral horn ipsilateral to the injury, (D) ventral horn contralateral to the injury. \* $P < 0.05$ , significant difference from other examined time points.



**Figure 11.** Comparisons of (A) CGRP-IR area ratios at the same time point post-surgery between the dorsal horns and (B) CGRP-expressing cells between the ventral horns. \* $P < 0.05$ , significant difference from other examined locations.

proper biomaterials to fabricate the artificial guides, such as silicone rubber,<sup>[38,39]</sup> collagen,<sup>[40,41]</sup> gelatin,<sup>[42,43]</sup> polylactates,<sup>[25,44]</sup> polycaprolactone,<sup>[45]</sup> and so on. In this study, for the first time, we proved that the casein crosslinked by glutaraldehyde was suitable for application as artificial nerve conduits.

Due to its excellent mechanical properties, the GCC conduits were successfully prepared. The GCC conduits had uniform and compact wall microstructures which could prevent the connective and scar tissues from growing into the internal lumen to hinder the nerve regeneration. In addition, the GCC did not induce cytotoxic effects to the cultured Schwann cells, which had a good hydrophilicity and could keep its integrity even after 80 h of soaking in the de-ionized water. The non-invasive real-time NF- $\kappa$ B bioluminescence imaging accompanied with histochemical assessment also showed the GCC was highly biocompatible, only evoking a mild tissue response. These results are not surprising since casein has been shown as a promising material for use in drug delivery,<sup>[46]</sup> and glutaraldehyde has shown prominent cross-linking capability for artificial organs including bones, corneas, skins, and nerves.<sup>[47–50]</sup>

From in vivo observations, we found that the GCC conduits did not display any unsatisfactory swelling or deformation during the long in vivo implant period after

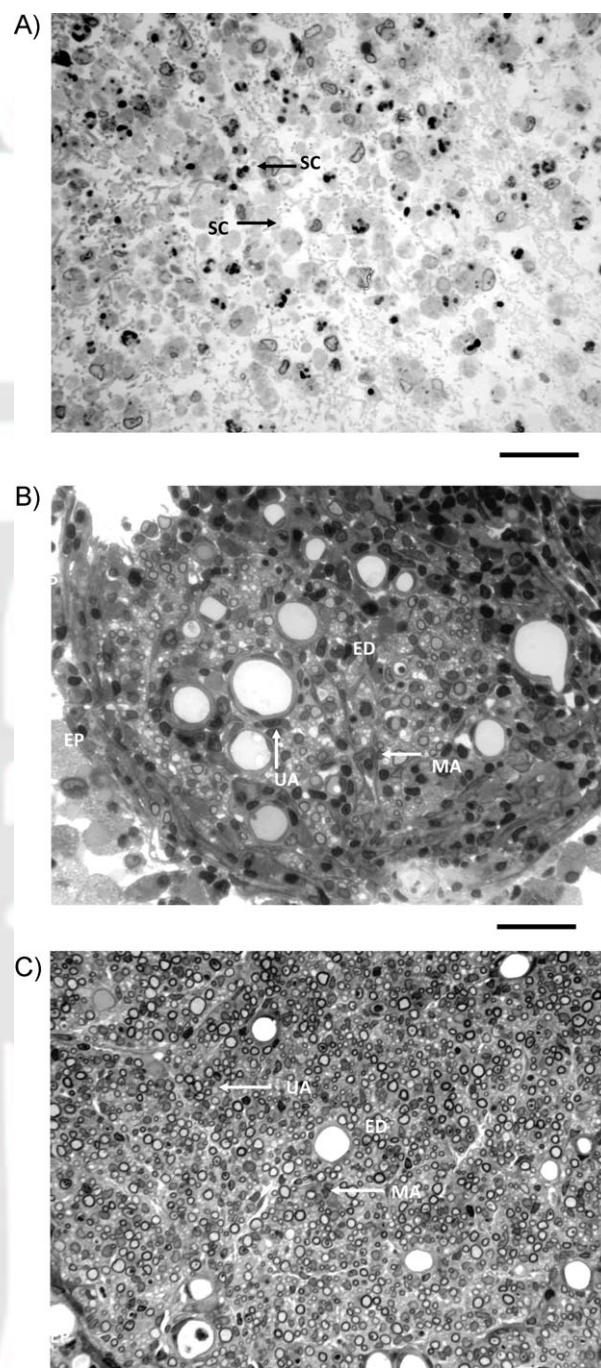


**Figure 12.** Light micrographs of regenerated nerve cross-sections at different implantation periods, (A) 2 weeks, (B) 5 weeks, and (C) 8 weeks. At 2 weeks, regenerated nerves were only composed of fibrin matrices populated by Schwann cells (SC). After 5 weeks, myelinated (MA) and unmyelinated axons (UA) had been seen in the endoneurium (ED) surrounded by the epineurium (EP). Scale bars: 100  $\mu$ m.

surgery. The stable dimensions of the GCC conduits could result from the chemical crosslinking of glutaraldehyde with the amino groups on the casein macromolecular

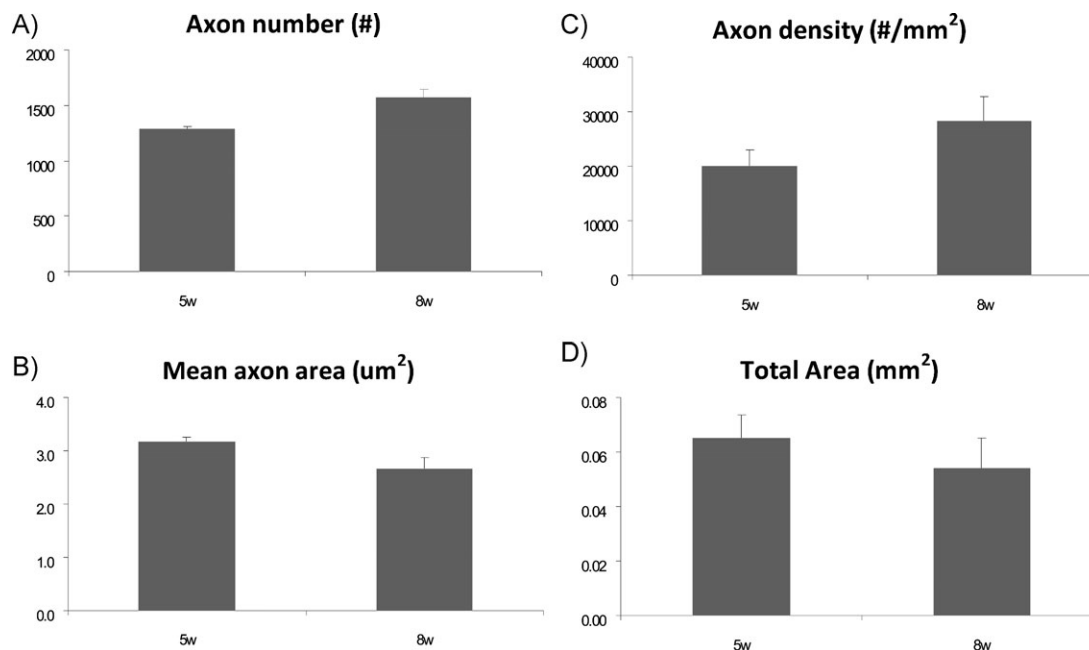


Figure 13. Morphometric analysis from the regenerated nerves in the GCC conduits, including (A) axon number, (B) axon area, (C) axon density, and (D) total nerve area. \* $P < 0.05$ , significant difference from other examined time points.

1 chains.<sup>[51]</sup> Healthy growth of nerve tissue was observed in  
 2 all conduits, again confirming the good biocompatibility of  
 3 GCC to nerve tissue. MAPs are thought to reappear when  
 4 regenerating myelinated nerve fibers have reached their  
 5 target organ.<sup>[52–54]</sup> The electrophysiological indexes,  
 6 including amplitude, latency, duration, and NCV of the  
 7 regenerated nerves were improved as a function of the  
 8 experimental period which could be attributed to the quick  
 9 recovery of nerve conducting function in the implanted  
 10 rats. In addition, histological assessment showed that the  
 11 temporal and spatial progresses of cellular activity within  
 12 the GCC conduits are similar to those seen for experiments  
 13 using artificial guides for peripheral nerve regeneration  
 14 reported in the literature.<sup>[33,55]</sup> At 2 weeks post-surgery,  
 15 fibrin matrices had formed in the GCC conduits, providing a  
 16 framework for subsequent migration of fibroblasts,  
 17 Schwann cells, and axons from the severed ends. After  
 18 5 weeks of regeneration, myelinated axons had grown  
 19 across the gap, indicating the GCC conduit could offer a  
 20 beneficial environment to the growing axons. These  
 21 histological results were supported by the protein levels  
 22 of CGRP in associated spinal cord segments, which were  
 23 gradually decreased during the test period. Since the CGRP  
 24 has been recognized as a nerve regeneration-promoting  
 25 peptide *in vivo*,<sup>[56–58]</sup> it can therefore be surmised that  
 26 when regenerating nerves becomes more mature, the CGRP  
 27 expression in the spines may decline and return to normal  
 28 values as a consequence of reconnection of the two severed  
 29 nerve stumps.

1 Finally, the quantitative data in several recent studies on  
 2 biodegradable bridging conduits to repair injured rat sciatic  
 3 nerves were gleaned from the literature. It is noted that the  
 4 quantitative data in the regenerated nerves in the GCC  
 5 conduits (myelinated axon density =  $28\,000 \cdot \text{mm}^{-2}$ ) are  
 6 about in the same range or even better than those in  
 7 most of the biodegradable conduits, such as chitosan  
 8 ( $15\,300 \cdot \text{mm}^{-2}$ ),<sup>[59]</sup> polylactic acid (mostly unmyelinated  
 9 axons),<sup>[3]</sup> polyglycolic acid ( $15\,300 \cdot \text{mm}^{-2}$ ),<sup>[60]</sup> collagen  
 10 ( $38\,100 \cdot \text{mm}^{-2}$ ),<sup>[61]</sup> proanthocyanidin cross-linked gelatin  
 11 (mostly unmyelinated axons),<sup>[62]</sup> and the genipin cross-  
 12 linked gelatin (mostly unmyelinated axons).<sup>[62]</sup> In addition,  
 13 the temporal and spatial progresses of cellular activity  
 14 within the GCC conduit are similar to those seen for  
 15 experiments using silicone rubber nerve guides,<sup>[42,63]</sup>  
 16 which have largely been used in clinical practice. These  
 17 results show the casein crosslinked by glutaraldehyde could  
 18 be a potential material for application as artificial nerve  
 19 conduits.

## Conclusion

20 The current study is the first work dedicated to GCC, a newly  
 21 devised biodegradable nerve bridge. Combined with  
 22 the superior properties including strong mechanical  
 23 microstructure, high biocompatibility, no toxicity, as well  
 24 as good applicability for nerve regeneration together with  
 25 excellent electrophysiological progress, the casein based

1 conduits can be effectively used for peripheral nerve  
2 damage repair.

3 Acknowledgements: This research is supported in part by China  
4 Medical University and Hospital (CMU99-EW-03; DMR99-075) and  
5 Taiwan Department of Health Clinical Trial and Research Center of  
6 Excellence (DOH100-TD-B-111-004). We also would like to thank  
7 Dr. Tin-Yun Ho for the experimental help.  
8

9 Received: December 18, 2010; Revised: March 18, 2011; Published  
10 online: DOI: 10.1002/mabi.201000498  
11

Keywords: biocompatibility; biodegradable; crosslinking;  
strength

- 12 [1] C. C. Yeh, Y. C. Lin, F. J. Tsai, C. Y. Huang, C. H. Yao, Y. S. Chen,  
13 *Neurorehabil. Neural Repair* **2010**, *24*, 730.  
14 [2] M. C. Lu, C. H. Yao, S. H. Wang, Y. L. Lai, C. C. Tsai, Y. S. Chen,  
15 *J. Trauma* **2010**, *68*, 434.  
16 [3] M. C. Lu, C. C. Tsai, S. C. Chen, F. J. Tsai, C. H. Yao, Y. S. Chen,  
17 *J. Trauma* **2009**, *67*, 1066.  
18 [4] J. Y. Chang, T. Y. Ho, H. C. Lee, Y. L. Lai, M. C. Lu, C. H. Yao, Y. S.  
19 Chen, *Artif. Organs* **2009**, *33*, 1075.  
20 [5] P. Pliikk, S. Målberg, A. C. Albertsson, *Biomacromolecules* **2009**,  
21 *10*, 1259.  
22 [6] L. Thomsen, P. Bellemere, T. Loubersac, E. Gaisne, P. Poirier,  
23 F. Chaise, *Chir. Main.* **2010**, *29*, 255.  
24 [7] M. Merle, A. L. Dellon, J. N. Campbell, P. S. Chang, *Microsurgery*  
25 **1989**, *10*, 130.  
26 [8] R. Birch, *Hand* **1979**, *11*, 211.  
27 [9] I. V. Yannas, B. J. Hill, *Biomaterials* **2004**, *25*, 1593.  
28 [10] W. N. Eigel, C. J. Hofmann, B. A. Chibber, J. M. Tomich, T. W.  
29 Keenan, E. T. Mertz, *Proc. Natl. Acad. Sci. USA* **1979**, *76*, 2244.  
30 [11] W. R. Aimutis, E. T. Kornegay, W. N. Eigel, *J. Dairy Sci.* **1982**, *65*,  
31 1874.  
32 [12] G. F. Chi, M. R. Kim, D. W. Kim, M. H. Jiang, Y. Son, *Exp. Neurol.*  
33 **2010**, *222*, 304.  
34 [13] H. Liu, Y. Kim, S. Chattopadhyay, I. Shubayev, J. Dolkas, V. I.  
35 Shubayev, *J. Neuropathol. Exp. Neurol.* **2010**, *69*, 386.  
36 [14] J. Wang, P. Zhang, Y. Wang, Y. Kou, H. Zhang, B. Jiang, *Artif.*  
37 *Cells Blood Substit. Immobil. Biotechnol.* **2010**, *38*, 24.  
38 [15] T. Y. Ho, Y. S. Chen, C. Y. Hsiang, *Biomaterials* **2007**, *28*, 4370.  
39 [16] C. Y. Hsiang, Y. S. Chen, T. Y. Ho, *Biomaterials* **2009**, *30*, 3042.  
40 [17] A. Loesch, H. Tang, M. A. Cotter, N. E. Cameron, *Angiology*  
41 **2010**, *61*, 651.  
42 [18] E. Adeghate, H. Rashed, S. Rajbandari, J. Singh, *Ann. N. Y. Acad.*  
43 *Sci.* **2006**, *1084*, 296.  
44 [19] X. Q. Li, V. M. Verge, J. M. Johnston, D. W. Zochodne,  
45 *J. Neuropathol. Exp. Neurol.* **2004**, *63*, 1092.  
46 [20] International Standard ISO10993-5, Biological Evaluation of  
47 Medical Devices. Part 5: Tests for Cytotoxicity: In Vitro  
48 Methods **1992**.  
49 [21] L. F. Zheng, R. Wang, Y. Z. Xu, X. N. Yi, J. W. Zhang, Z. C. Zeng,  
50 *Brain Res.* **2008**, *1187*, 20.  
51 [22] X. Wang, L. Sang, D. Luo, X. Li, *Colloids Surf. B, Biointerfaces*  
52 **2011**, *82*, 233.  
53 [23] A. Sionkowska, J. Skopinska-Wisniewska, M. Gawron,  
54 J. Kozłowska, A. Planecka, *Int. J. Biol. Macromol.* **2010**, *47*, 570.  
55 [24] C. Huang, R. Chen, Q. Ke, Y. Morsi, K. Zhang, X. Mo, *Colloids*  
56 *Surf. B, Biointerfaces* **2011**, *82*, 307.  
57 [25] M. Sun, S. Downes, *J. Mater. Sci. : Mater. Med.* **2009**, *20*, 1181.  
58 [26] W. Wang, S. Itoh, A. Matsuda, S. Ichinose, K. Shinomiya,  
59 Y. Hata, J. Tanaka, *J. Biomed. Mater. Res. A* **2008**, *84*, 557.  
60 [27] M. F. Meek, K. Jansen, R. Steendam, W. van Oeveren, P. B. van  
61 Wachem, M. J. van Luyn, *J. Biomed. Mater. Res. A* **2004**, *68*, 43.  
62 [28] B. A. Harley, J. H. Leung, E. C. Silva, L. J. Gibson, *Acta Biomater.*  
63 **2007**, *3*, 463.  
64 [29] M. P. Prabhakaran, J. R. Venugopal, S. Ramakrishna, *Biomater-*  
65 *ials* **2009**, *30*, 4996.  
66 [30] L. Ghasemi-Mobarakeh, M. P. Prabhakaran, M. Morshed, M. H.  
67 Nasr-Esfahani, S. Ramakrishna, *Biomaterials* **2008**, *29*, 4532.  
68 [31] J. Pan, M. Zhao, Y. Liu, B. Wang, L. Mi, L. Yang, *J. Biomed. Mater.*  
69 *Res. A* **2009**, *89*, 160.  
70 [32] G. H. Borschel, K. F. Kia, W. M. Kuzon, R. G. Dennis, *J. Surg. Res.*  
71 **2003**, *114*, 133.  
72 [33] L. R. Williams, F. M. Longo, H. C. Powell, G. Lundborg, S. Varon,  
73 *J. Comp. Neurol.* **1983**, *218*, 460.  
74 [34] P. G. di Summa, P. J. Kingham, W. Raffoul, M. Wiberg,  
75 G. Terenghi, D. F. Kalbermatten, *J. Plast. Reconstr. Aesthet.*  
76 *Surg.* **2010**, *63*, 1544.  
77 [35] T. Matsuyama, M. Mackay, R. Midha, *Neurol. Med. Chir.*  
78 *(Tokyo)* **2000**, *40*, 187.  
79 [36] M. Rivlin, E. Sheikh, R. Isaac, P. K. Beredjickian, *Hand Clin.*  
80 **2010**, *26*, 435.  
81 [37] A. Klimczak, M. Siemionow, *Semin. Plast. Surg.* **2007**, *21*, 226.  
82 [38] M. D. Wood, D. Hunter, S. E. Mackinnon, S. E. Sakiyama-Elbert,  
83 *J. Biomater. Sci., Polym. Ed.* **2010**, *21*, 771.  
84 [39] M. Ishiguro, K. Ikeda, K. Tomita, *J. Orthop. Sci.* **2010**, *15*, 233.  
85 [40] S. Madduri, P. di Summa, M. Papaloizos, D. Kalbermatten,  
86 B. Gander, *Biomaterials* **2010**, *31*, 8402.  
87 [41] L. Yao, G. C. de Ruiter, H. Wang, A. M. Knight, R. J. Spinner, M. J.  
88 Yaszemski, A. J. Windebank, A. Pandit, *Biomaterials* **2010**, *31*,  
89 5789.  
90 [42] Y. C. Yang, C. C. Shen, T. B. Huang, S. H. Chang, H. C. Cheng, B. S.  
91 Liu, *J. Biomed. Mater. Res., B: Appl. Biomater.* **2010**, *95*, 207.  
92 [43] C. J. Chang, *J. Biomed. Mater. Res. A* **2009**, *91*, 586.  
93 [44] H. B. Wang, M. E. Mullins, J. M. Cregg, C. W. McCarthy, R. J.  
94 Gilbert, *Acta Biomater.* **2010**, *6*, 2970.  
95 [45] C. M. Valmikinathan, S. Defroda, X. Yu, *Biomacromolecules*  
96 **2009**, *10*, 1084.  
97 [46] A. J. Santinho, J. M. Ueta, O. Freitas, N. L. Pereira,  
98 *J. Microencapsul.* **2002**, *19*, 549.  
99 [47] M. B. Keogh, F. J. O'Brien, J. S. Daly, *Acta Biomater.* **2010**, *6*,  
100 4305.  
101 [48] E. Bentley, C. J. Murphy, F. Li, D. J. Carlsson, M. Griffith, *Cornea*  
102 **2010**, *29*, 910.  
103 [49] M. B. Dainiak, I. U. Allan, I. N. Savina, L. Cornelio, E. S. James,  
104 S. L. James, S. V. Mikhailovsky, H. Jungvid, I. Y. Galaev, *Bio-*  
105 *materials* **2010**, *31*, 67.  
106 [50] M. H. Chen, P. R. Chen, M. H. Chen, S. T. Hsieh, J. S. Huang, F. H.  
107 Lin, *J. Biomed. Mater. Res. B* **2006**, *77*, 89.  
108 [51] M. S. Latha, A. V. Lal, T. V. Kumary, R. Sreekumar,  
109 A. Jayakrishnan, *Contraception* **2000**, *61*, 329.  
110 [52] F. Werdin, H. Grüssinger, P. Jaminet, A. Kraus, T. Manoli,  
111 T. Danker, E. Guenther, M. Haerlec, H. E. Schaller, N. Sinis,  
112 *J. Neurosci. Methods* **2009**, *182*, 71.  
113 [53] N. Lago, F. J. Rodríguez, M. S. Guzmán, J. Jaramillo, X. Navarro,  
114 *J. Neurosci. Res.* **2007**, *85*, 2800.  
115 [54] H. Y. Chiang, H. F. Chien, H. H. Shen, J. D. Yang, Y. H. Chen, J. H.  
116 Chen, S. T. Hsieh, *J. Neuropathol. Exp. Neurol.* **2005**, *64*, 576.

- 1 [55] M. C. Lu, C. Y. Ho, S. F. Hsu, H. C. Lee, J. H. Lin, C. H. Yao, Y. S.  
2 Chen, *Neurorehabil. Neural Repair* **2008**, *22*, 367. 1  
3 [56] I. A. Belyantseva, G. R. Lewin, *Eur. J. Neurosci.* **1999**, *11*, 457. 2  
4 [57] A. Blesch, M. H. Tuszynski, *J. Comp. Neurol.* **2001**, *436*, 399. 3  
5 [58] L. J. Chen, F. G. Zhang, J. Li, H. X. Song, L. B. Zhou, B. C. Yao, F. Li,  
6 W. C. Li, *J. Clin. Neurosci.* **2010**, *17*, 87. 4  
7 [59] G. Wang, G. Lu, Q. Ao, Y. Gong, X. Zhang, *Biotechnol. Lett.* **2010**,  
8 *32*, 59. 5  
[60] T. Waitayawinyu, D. M. Parisi, B. Miller, S. Luria, H. J. Morton,  
S. H. Chin, T. E. Trumble, *J. Hand Surg. Am.* **2007**, *32*,  
1521. 6  
[61] B. S. Liu, *J. Biomed. Mater. Res. A* **2008**, *87*, 1092. 7  
[62] Y. S. Chen, J. Y. Chang, C. Y. Cheng, F. J. Tsai, C. H. Yao, B. S. Liu,  
*Biomaterials* **2005**, *26*, 3911. 8  
[63] F. Xie, Q. F. Li, B. Gu, K. Liu, G. X. Shen, *Microsurgery* **2008**, *28*,  
471. 9

1  
2  
3  
4  
5  
6  
7  
8  
9  
10

Q1: Author: Please clarify throughout the article all editorial/  
technical requests marked by black boxes.

\*: Author: Please note that Figure 4,5,6,8,9 and Figure for  
ToC and abstract will be printed in color.



WILEY-VCH



# Macromolecular Bioscience



## Reprint Order Form 2011 - please return with your proofs

<http://www.mbs-journal.de>  
<http://www.interscience.wiley.com>

Wiley-VCH  
Boschstrasse 12, 69469 Weinheim  
Germany  
Tel.: +49 (0) 6201 – 606 – 581  
Fax: +49 (0) 6201 – 606 – 309 or 510  
Email: [macromol@wiley-vch.de](mailto:macromol@wiley-vch.de)

Manuscript: mabi. \_\_\_\_\_

Author: \_\_\_\_\_

Please send me and bill me for

no. of **reprints** via  airmail (+ 25 Euro)  
 surface mail

Please send me and bill me for

no. of **copies of this issue**  
(1 copy: 20 Euro)  
via  airmail (+ 25 Euro)  
 surface mail

Please send me and bill me for

**high-resolution PDF file** (330 Euro). My e-mail  
address: \_\_\_\_\_

**Mail reprints / copies of the issue to:**

\_\_\_\_\_  
\_\_\_\_\_  
\_\_\_\_\_  
\_\_\_\_\_

**Send bill to:**

\_\_\_\_\_  
\_\_\_\_\_  
\_\_\_\_\_  
\_\_\_\_\_

Please note: It is not permitted to present the PDF file in  
the internet or on company homepages

My **VAT number** is (institutes / companies in EU  
countries only): \_\_\_\_\_

Invoices without VAT can only be processed with the  
VAT number of the institute / company. Please provide it  
with your order.

You will receive an invoice with your order.

**Payment by credit card:**



Card no. \_\_\_\_\_

Expiry date: \_\_\_\_ / \_\_\_\_

Date, Signature: \_\_\_\_\_

**Purchase Order Number:** \_\_\_\_\_  
(Please contact your administrative office if you need one)

### Price list for reprints

Postage and handling charges included. All Wiley-VCH prices are exclusive of VAT.

No. of pages	Price (in Euro) for orders of					
	50 copies	100 copies	150 copies	200 copies	300 copies	500 copies
1-4	330	385	425	445	548	752
5-8	470	556	608	636	784	1077
9-12	610	717	786	824	1016	1396
13-16	744	874	958	1004	1237	1701
17-20	885	1040	1138	1196	1489	2022
for every additional 4 pages	140	164	175	188	231	315